Modelling the functioning of a coupled microphytobenthic-EPS-bacterial system in intertidal mudflats

C. Rakotomalala, Katell Guizien, K. Grangeré, S. Lefebvre, C. Dupuy, F. Orvain

Modelling the functioning of a coupled Microphytobenthic-EPS-bacterial system in intertidal mudflats

Rakotomalala C [1*], Guizien K [2], Grangeré K [1], Lefebvre S [3], Dupuy C [4], Orvain F [1]

Abstract

A mechanistic and biogeochemical model was developed to analyze the interactions between microphytobenthos (MPB), bacteria and nutrients in a tidal system. Behavioral vertical migration was hypothesized as being controlled by exogenous factors (tide and light) but also by endogenous factors (carbon and nitrogen requirements). The secretion of Extracellular Polymeric Substances (EPS) during photosynthesis (overflow metabolism) and migration of diatoms was also formulated. Similarities in MPB dynamics between observations and simulations support the assumption that carbon and nitrogen ratios are additional key processes behind the vertical migration of diatoms in the sediment. The model satisfactorily reproduced the three growth phases of the MPB development observed in a mesocosm (the lag phase, the logarithmic growth, and the plateau). Besides, nutrient availability, which could be induced by faunal bioturbation, significantly determined the extent of MPB biomass and development. The plateau phase observed in the last days of simulations appeared to be attributed to a nutrient depletion in the system, emphasizing the importance of nutrient availability. The model, although improvable especially on the formulation of the EPS excretion and bacteria development, already updated understanding of several aspects of benthic-system functioning during experimental conditions.

Key words: Microphytobenthos, migration, carbon and nitrogen ratio, biogeochemical model

Highlights:

- A biogeochemical model of a benthic system was developed
- A focus on MPB primary production was investigated in model simulations
- This study highlighted that internal C/N ratio plays a key role in the MPB development
- Nitrogen availability is a driver of MPB migration and production

Declarations of interest: none

[1] Université de Caen Basse-Normandie, UMR BOREA, MNHN, UPMC, UCBN, CNRS-7208, IRD-207, Laboratoire de Biologie des Organismes et Ecosystèmes Aquatiques, Esplanade de la Paix, 14032 Caen, France (Corresponding author) Email : rakotomalala.c@gmail.com

* *Corresponding author: rakotomalala.c@gmail.com*

[2] Université Paris 06-CNRS, UMR 8222, LECOB, Laboratoire d'Ecogéochimie des Environnements Benthiques, rue du Fontaulé, F-66650, Banyuls/mer, France
[3] Université de Lille, CNRS, Université du Littoral Côte d'Opale, UMR 8187, LOG, Laboratoire d'Océanologie et de Géosciences, F-62930 Wimereux, France
[4] Université de la Rochelle-CNRS, UMR 7266, Littoral Environnement et Sociétés (LIENSs), 2 rue Olympe de Gouges, 17000 La Rochelle cedex, France

Corresponding author: Dr Christiane Rakotomalala
Email of corresponding author: rakotomalala.c@gmail.com

* *Corresponding author: rakotomalala.c@gmail.com*

1. Introduction

A significant part of the primary production in estuarine systems is sustained by microphytobenthos (MPB) (Cloern et al., 2014; Underwood and Kromkamp, 1999) which photosynthetic activity takes place within a thin layer of the sediment (photic zone) with less than 1mm thickness in muddy substrata (Kromkamp et al., 1998; Serôdio et al., 1997). MPB can be resuspended in the water column and contributes to planktonic biomass (de Jonge and Van Beusekom, 1992; Ubertini et al., 2015) making benthic-pelagic coupling a critical process in coastal systems. Consequently, MPB constitutes major contributor to carbon and energy flow within food webs in intertidal zones (Gaudron et al., 2016) and subtidal zones (Kang et al., 2015).

Epipelic diatoms, denominated as MPB in this study, represent the dominant constituent of benthic microautotrophs in muddy flats (Barranguet et al., 1996). It is assumed that growth of MPB in the sediment is temporally restricted to few hours during diurnal low tides (Guarini et al., 2000a), a period which is characterized by extreme variations of environmental factors. Temperature may reach more than 40°C in summer during midday emersion in some location and can have deleterious impact on benthic microalgae growth (Béchet et al., 2017; Blanchard et al., 1996). MPB functioning is well adapted to such extreme conditions such as vertical migration (Consalvey et al., 2004) and/or physiological photoprotection to excessive light (Barnett et al., 2015). Development of benthic diatoms in the sediment is accompanied by production of mucilaginous substances, commonly denominated as "Extracellular Polymeric Substances" (EPS) predominantly composed of carbohydrates which was reported to facilitate the migration of cells (Smith and Underwood, 1998). The EPS also have role in retaining moieties through hydrophilic properties (McKew et al., 2011) and in sediment physical properties protecting against sediment erosion (Underwood and Paterson, 1993). Furthermore, EPS secretion can fuel the bacterial compartment (Agogué et al., 2014).

Despite the knowledge on MPB and its importance in coastal ecosystems, specific model of MPB development remains scarce compared to phytoplankton (Bernard, 2011; Geider et al., 1998; Ross and Geider, 2009; Shimoda and Arhonditsis, 2016). This induced the use of phytoplanktonic-adapted models to simulate the microphytobenthic compartment (Blackford, 2002; Hochard et al., 2010). Models describing MPB development using forcing factors such as light and tide (Pinckney and Zingmark, 1993; Savelli et al., 2018; Serôdio and Catarino, 2000) or light, temperature and hydrodynamic disturbances (Mariotti and Fagherazzi, 2012) were developed. Specific behavioral and physiological adaptations of benthic microalgae were

* *Corresponding author: rakotomalala.c@gmail.com*

rarely taken into account albeit the model developed by Guarini et al. (2000b) which remains a reference model to date. Vertical migration, a key process in MPB functioning, is based on a chronobiological behavior induced by two exogenous factors namely tide and light in the study of Guarini et al. (2000b) as demonstrated by several studies (Consalvey et al., 2004; de Brouwer and Stal, 2001; Mitbavkar and Anil, 2004). However, exogenous factors alone may not be sufficient to explain the MPB vertical migration as resuspension of MPB has been observed without sediment erosion (Guarini et al., 2008; Mariotti and Fagherazzi, 2012) and vertical migration of MPB in the subtidal zone have been attributed to endogenous factors (Ní Longphuirt et al., 2009). In addition, analyzes conducted by Kingston (2002) revealed a downward migration stimulated by nutrient supply which could be enhanced by faunal bioturbation (D'Hondt et al., 2018; Swanberg, 1991). Vertical migration could, therefore, be controlled by internal requirements, either in terms of carbon at the surface with light or in terms of nitrogen deeper at potentially nutrient-enriched sediment (Kingston, 2002). It is thus important to respond to the lack of models integrating the critical processes of MPB development. There is also a clear challenge in incorporating the nitrogen cycle and diagenetic mechanisms for better simulating the primary production of MPB and exchanges of carbon and nitrogen with other elements of the biogeochemical cycle at the sediment-water interface (Hochard et al., 2012).

The purpose of this study was to analyze the functioning of a benthic system composed of epipelic diatoms and bacteria using a biogeochemical model which integrated critical features of MPB development in the sediment. Precisely, this study explored the hypothesis that MPB vertical migration is controlled by both endogenous factors (carbon and nitrogen requirements) and exogenous factors (light and tide). Moreover, EPS metabolic routes during photosynthesis and vertical migration of MPB (de Brouwer et al., 2006; Smith and Underwood, 2000; Staats et al., 2000) were modelled and analyzed. MPB development was analyzed under different extents of nutrients. The dynamics of MPB development and EPS production measured during a 10-day experiment in a tidal mesocosm were used to evaluate the model. Sensitivity analyses of the model were also performed.

2. Material and methods

2.1. Model description

The model developed herein is based on MPB model of Guarini et al (2000b) and on phytoplankton quota model of Geider et al. (1998). Quota models were specifically dedicated to account for dynamic C/N ratios in phytoplankton (see Ross and Geider 2009 and references

* Corresponding author: rakotomalala.c@gmail.com

therein) and consist in a system of 4 ordinary differential equations (functional and reserve carbon, nitrogen and chl *a* content). We adopted a simpler modeling strategy by using nitrogen as the basic unit and carbon, involved in MPB photosynthesis, as an accessory variable but in two separate ODEs with a C/N ratio expected to be lower compared to that of Ross and Geider (2009).

The assimilation of nitrogen and the respiration of carbon were assumed to occur in the modelled photic and aphotic layers while the assimilation of carbon through photosynthesis only took place in the photic layer at low tide during daylight. Such dissociation of carbon metabolism with light and nitrogen metabolism with and without light have been also highlighted by Jauzein et al. (2011) for phytoplankton. Consequently, MPB was modeled as photosynthetically active (Dact:C and Dact:N) and inactive (D:C and D:N) biomass. Tide (6h low tide with light -18h high tide in the dark), ambient temperature (ca 16°C), and constant light (140 µmol photons m^{-2} s^{-1}) were the forcing variables of the model. CO_2 was not modeled as it was considered as non-limiting in the system. Upward migration was supposed to be driven by light, tide, and carbon requirements, while downward migration was only controlled by nitrogen requirements. At the surface, the benthic diatoms assimilated carbon during photosynthesis and nitrogen until carbon was in excess compared to nitrogen content (threshold value qC2N ca~3.5). Inversely, in the aphotic layer, diatoms assimilated nitrogen and respired carbon until the carbon content became insufficient (threshold value qN2C ca~1) then moved upward at low tide and in the presence of light. In this study, photosynthesis was limited only by light and temperature in the photic zone, nitrogen limitation provoking migration down the aphotic zone.

Processes, such as EPS production by benthic diatoms and interaction with bacteria, were recently integrated in a biogeochemical model (Hochard et al., 2010). Some authors highlighted the excretion of EPS by diatom cells related to an overflow metabolism, adhesion, and locomotion (de Brouwer et al., 2006; Orvain et al., 2003; Smith and Underwood, 1998). Exudation of EPS during photosynthesis was integrated in the model as Dissolved Organic Carbon (DOC). Conversely, EPS release during vertical migration was also modelled as a release of dissolved organic nitrogen (DON) and a loss of carbon outside the system.

In the present model, bacteria development was simply integrated and limited by the availability of DON. An inhibition effect of EPS (DOC) on bacterial development in the biofilm (Agogué et al., 2014; Doghri et al., 2017) was also taken into account. Bacterial mortality was attributed to viral lysis (Le Chevanton et al., 2013; Siem-Jørgensen et al., 2008).

* *Corresponding author: rakotomalala.c@gmail.com*

Simple formulations were adopted to represent the mineralization of PON (Particulate Organic Nitrogen) into DON and DON into DIN (Dissolved Inorganic Nitrogen: NH_4^+, NO_3^-, and NO_2^-). For now, the processes of nitrification/denitrification in relation to oxygen consumption were not detailed in this model, because the model was simplified to be in line with the dataset available for comparison. Moreover, this study focused on innovative mechanisms linking vertical migration to the C/N internal balance of MPB and not on the detailed dynamics of oxygen, ammonium and nitrates as this is the case in other models of MPB primary production in relation with early diagenesis of organic matter (Hochard et al., 2012, 2010).

The concept and processes integrated in the model were summarized in the Fig. 1. Details on model equations and parameters were developed in the appendix. The model developed herein was implemented in the numerical tool Eco3M (Baklouti et al., 2006). The code was developed in FORTRAN 90-95 and used Euler explicit method as solving methods. The code was under Cecill License.

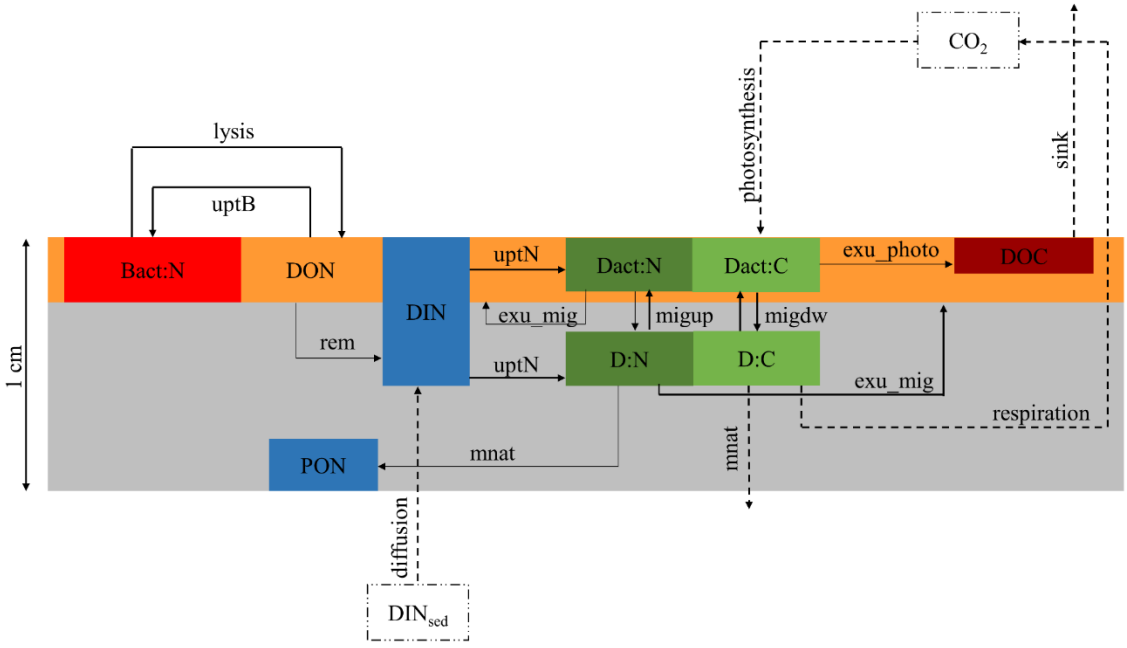

Fig. 1: Conceptual framework of the model of a benthic system constituted by MPB, Bacteria and nutrients in the first centimeter of sediment expressed in carbon and nitrogen respectively. MPB is distributed in active (Dact:N and Dact:C) or inactive layers (D:N and D:C). An overflow of carbon (DOC) is secreted during photosynthesis. Vertical migration represents the link between the two compartments, during which glycoproteins are secreted and directly fuel the first nutrient compartment (Dissolved Organic Nitrogen or DON). Bacteria (Bact:N) relies

* Corresponding author: rakotomalala.c@gmail.com

on DON and which development is inhibited by the photosynthesis-related carbon excretion DOC. Dissolved Inorganic Nitrogen (DIN), on which the MPB relies on, represents the second nutrient compartment. The Particulate Organic Nitrogen (PON) resulted from natural mortality of MPB cells. The scale of the boxes in the graph is not representative of reality. Sinks are represented by dashed arrows. Forcing variables are represented by dashed boxes.

2.2. Test case: the mesocosm study of Orvain et al. (2003)

Model performance was tested in comparison with the experimental study of Orvain et al., (2003) which analyzed the dynamics of benthic diatoms and associated extracellular carbohydrates excretion. In this experimental study, a natural community of diatoms was maintained in controlled conditions consisting of 6h diurnal low tide and 18h nocturnal high tide during 10 days in two different tanks. Erosion of sediment and MPB during rising and ebb tides were avoided in the mesocosm experiments (Orvain et al., 2003). Both processes were thus not integrated in the model. The mesocosm was maintained at ambient temperature (ca 16°C) and constant irradiance (PAR=140 µmol photons m^{-2} s^{-1}) during diurnal phases. Sediment was sieved through 1mm mesh prior to diatoms culture to remove macrofauna. However, meiofauna (nematoda and foraminifera) were still present in the sediment. Chl *a* and EPS (Low and High Molecular Weight) contained in the 1 cm of sediment were assayed at the beginning of diurnal emersion and just before diurnal immersion during 10 days. Each assay in each tank were performed in triplicate. Nutrients (urea, ammonium, nitrate/nitrite and phosphate) content was also measured at the beginning and at the end of the experiments over the first and the second centimeter depth.

2.3. Sensitivity analysis

2.3.1. Initial conditions

Values of photosynthetically active microphytobenthic biomasses (Dact:C and Dact:N) and the photosynthesis-related EPS (DOC) compartments were set to zero with the assumption that neither photosynthesis nor EPS production have taken place at the beginning of the experiments. As the silty mud (100% of fine mud <63µm) was collected *in situ* and manipulated thereafter, the algal cells were supposed to be in the state of carbon excess as after an emersion phase (C/N = 1.94:0.1). Two other MPB initial states were tested and related simulations were presented in supplementary material (SM1). The value of ammonium and nitrate recorded at the beginning of the experiment, expressed in the same unit as in the model, was used as initial values of DIN compartment in the first centimeter (0.343 mol N m^{-3}). As neither bacteria, nor DON, nor PON were assessed during the experiments and as the model appears not to be sensitive on the

* Corresponding author: rakotomalala.c@gmail.com

variation of the initial conditions of those three compartments, values were set arbitrary to 1, 0, and 5 mol N m^{-3} respectively as initial conditions.

2.3.2. Nutrient diffusion

At the beginning as well as at the end of the experiments of Orvain et al., (2003), concentrations of DIN (ammonium, nitrite, and nitrate) were higher in the second centimeter (0.563 to 0.312 mol N m^{-3} respectively) than in the first centimeter (0.343 to 0.036 mol N m^{-3}). Nutrient diffusion from deeper layers was likely going on in the experiments and has been already modelled in another study (Hochard et al., 2010). The hypothesis that nutrient input maintaining the growth of diatoms until the 10^{th} day could arise from the deeper layer was then tested. Diffusion of nutrients (DIN) controlled by the gradient known as Fickian chemical diffusion, between the deeper layer and the first centimeter of sediment, was thus integrated in the model (Scenario A) as in Lavery et al. (2001). Moreover, solute fluxes depending on sediment porosity and tortuosity (Boudreau, 1996) were also integrated in the Fickian formulation of the present study (Appendix Table 4). The DIN in the second centimeter was hypothesized to linearly decrease from the value at the beginning of the mesocosm culture (0.563 mol N m^{-3}).

Ecological role of meiofauna was reviewed (Schratzberger and Ingels, 2018) mentioning nutrient input and enhanced nutrient cycling due directly or indirectly to meiofauna functioning, which enhance diatoms development (D'Hondt et al., 2018). The paucity of studies quantifying the whole nutrient increase in the sediment due to meiofauna prompted us to test some values to integrate the processes. Two levels of biodiffusion simulations were thus tested by multiplying the diffusion coefficient by a factor 5 (Scenario B) and a factor 10 (Scenario C). Equation and parameters of diffusion were given in the appendix (Table 4 and 5).

2.3.3. C/N ratio threshold values

Sensitivity analysis of the intra-cellular quota C/N thresholds triggering the upward (qC2N=3.5) and downward (qN2C=1) migration was also conducted. The two parameters were varied about -50%, -30%, +30%, and +50%.

2.4. Statistical tests

The Taylor diagram (Taylor, 2001) was used to evaluate the performance of the model, which graphically groups the correlation between simulations and observations, the RMS error represented by the radial distance from the observation, and the standard deviation of the

* Corresponding author: rakotomalala.c@gmail.com

dynamics represented by the radial distance from the origin. Simulations with high value of the correlation coefficient, low value of the RMS error as well as dispersion equivalent to the observations reflects a very good fit. The experimental measurements of chl *a* and EPS from the study of Orvain et al. (2003) were converted in carbon concentration using ratios of C/chl *a* = 45 and Glucose/C = 15.

3. Results

3.1. Functioning of the benthic system model

Vertical migration of MPB was simulated and depicted by upward migration to the active layer at the beginning of nearly each diurnal emersion and downward migration to the inactive layer until dark immersion (Fig. 2a and e). Precisely, carbon requirement brought cells to the surface to accumulate carbon until the later became in excess then nitrogen requirement induced them to go back to the sediment, where carbon content progressively decreased through respiration while nitrogen content increased. Carbon and nitrogen transfers between active (Fig. 2a) and inactive layers (Fig. 2e) were reproduced by an inverse pattern between them. The 6 first days, both N/C and C/N ratio in the inactive and active layer (Fig. 2c green and black line) exceeded the threshold values (qN2C = 1 and qC2N = 3.5) respectively resulting in daily upward and downward migration of cells (Fig. 2a and e). Diatom migration from the inactive to the active layer occurred when cells were nitrogen enriched (Fig. 2c green line) except for the day 6, 9, and 10. The exponential development of diatoms was modelled at the surface as depicted by the abrupt increase in the carbon content of MPB (black line) after 6 days of latency and moderate growth period (Fig. 2a). Diatoms remained at the surface during 2 days then MPB growth drastically dropped to literally stop thereafter resulting in an empty active layer (Fig. 2a) and a maximum concentration of carbon and nitrogen in the inactive layer the last two days (Fig. 2f).

* *Corresponding author: rakotomalala.c@gmail.com*

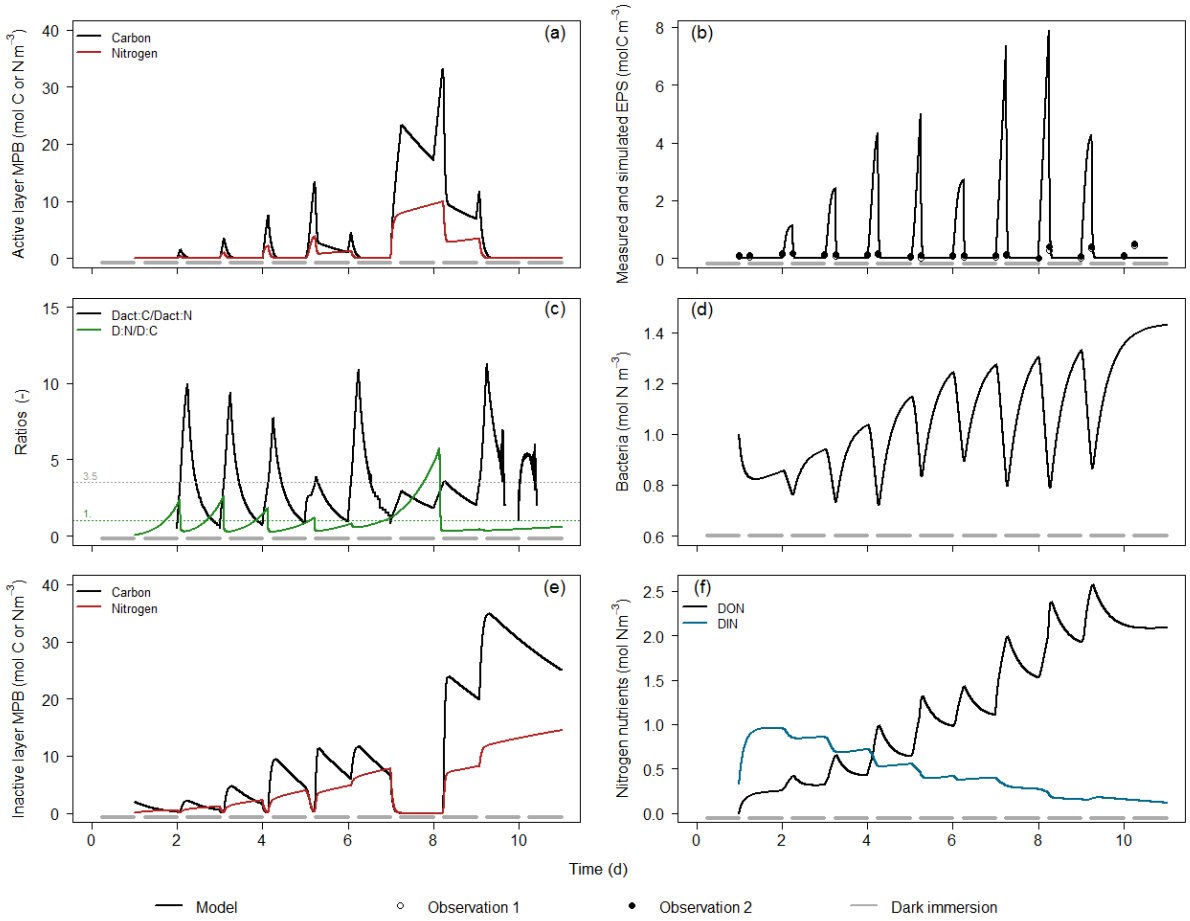

Fig.2: Simulated functioning of the benthic system. Temporal dynamics of: (a, e) the carbon (black line) and the nitrogen (blue line) concentrations of MPB in the active (a) and inactive (e) layers; (b) the photosynthesis-related DOC (line) confronted with the measured EPS HMW (points); (c) the C/N ratio in the active layer (black) and the N/C ratio in the inactive layer; (d) the bacterial biomass, (f) the dissolved inorganic nitrogen DIN (red) and the dissolved organic nitrogen DON (black) in the first centimeter of sediment. Gray line in each graph represents dark immersion periods in the system while space in between represents emersion phase with light.

While DIN availability overall decreased in the system until near-depletion, both bacterial biomass and DON increased (Fig. 2d and f black). All three compartments (DIN, bacterial nitrogen content and DON) exhibited daily oscillations. During the 6 hours of diurnal emersion when MPB was photosynthetically active, bacterial biomass and DIN decreased while DON increased. During 18 hours dark immersion, decrease of DON concentration (Fig. 2f black) was observed whereas inverse pattern was simulated for bacteria (Fig. 2d black). At the same time,

* Corresponding author: rakotomalala.c@gmail.com

290 DIN concentration (Fig. 2f blue) slightly increased during 6 days and decreased thereafter when
291 maximum concentration of nitrogen in the inactive layer was observed.

292 It was noteworthy that biomass of bacterial decline during diurnal emersion was
293 proportional to the DOC increase (Fig. 2b line), as expected from bacterial growth inhibition
294 by DOC. However, as soon as DOC was hydrolyzed during immersion, bacterial growth
295 outcompeted viral lysis of bacteria and bacterial biomass increased again. DOC variation
296 followed photosynthetic activity depicted by active diatom carbon content, and therefore the
297 DOC increase was larger in days 7 and 8 than during the 6 days of latency and moderate growth
298 period. This was only partially in agreement with pronounced increase of EPS-HMW (Fig. 2b
299 points) observed the 3 last days in Orvain et al. (2003) experiments. Moreover, the extent of
300 simulated DOC was largely higher compared to observed EPS concentrations.

301 **3.2. Sensitivity analysis**

302 **3.2.1. Nutrient availability**

303 In the mesocosm study by Orvain et al. (2003), the temporal variation of MPB growth
304 showed 3 distinct phases of development. The lag phase lasted about 3 days and was followed
305 by continuous increase being the greatest between the 8^{th} and the 9^{th} day and stabilized over the
306 last day (Fig. 3, points).

307 Dynamics of modelled carbon in the 1^{st} cm of sediment (pooling active and inactive layers)
308 over the 10 days simulation was substantially lower when integrating chemical diffusion alone
309 (Fig. 3 blue curve). When diffusion was limited to Fickian diffusion, the model underestimated
310 the MPB biomass as illustrated by RMSE higher than 10 (Fig. 3, left graph, blue point). The lag
311 phase was well reproduced however the two last phases of MPB growth during an experimental
312 configuration were not reproduced. Simulated pattern showed lower correlation with observed
313 patterns (R~0.6) and low standard deviation (~2 mol C m^{-3}) reflecting lower spatial variability.

314 With a biodiffusion of nutrients 5 times greater than the Fickian diffusion, concentration of
315 carbon was higher than simulations conducted with chemical diffusion (Fig. 3 cyan curve).
316 Enhanced nutrient availability resulted in daily growth of MPB with a cyclic succession of high
317 production followed by lower production the next day. The exponential phase happened one
318 day later compared to observations. The model did not fit well the observed pattern during the
319 6h productive period (Fig. 3, left graph, cyan point) with lower spatial variability depicted by
320 low standard deviation (~8 mol C m^{-3}) compared to standard deviation of measurements (~12

* Corresponding author: rakotomalala.c@gmail.com

mol C m^{-3}). However, simulated pattern was closer to data than the previous simulation with better correlation (R~0.87) and lower RMSE (~6).

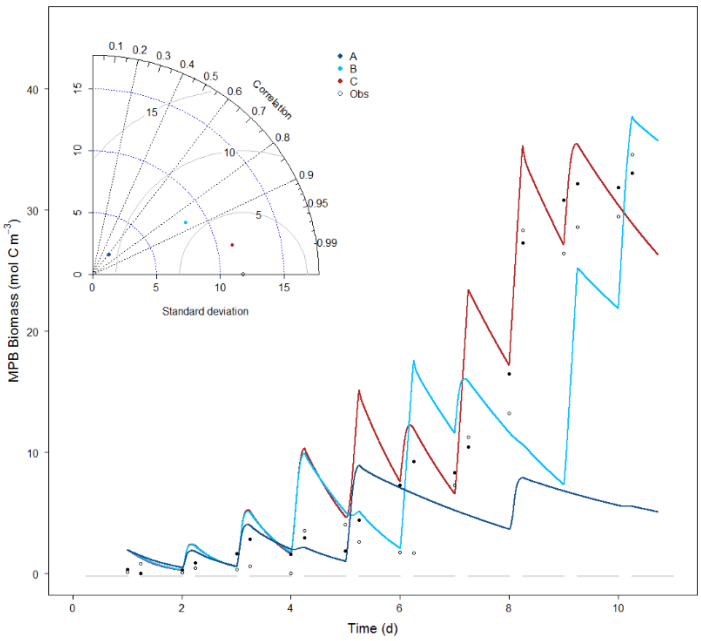

Fig. 3: Simulated MPB biomass (lines) in the first centimeter of sediment under three different extent of diffusion: chemical diffusion (blue), and bio-diffusion 5 times (cyan) and 10 times (red) greater than the chemical diffusion. The points represent the MPB biomass calculated from the study of Orvain et al. (2003). Gray line represents dark immersion periods in the system. The left graph represents the Taylor diagram showing the difference between the observed MPB and the simulated MPB under three different diffusion extent. Gray and blue dashed curves represent respectively the RMSE and the standard deviation of observed and simulated dynamics.

With enhanced refueling of DIN compartment (10 times the chemical diffusion), the dynamics of the MPB (Fig. 3, red curve) was similar to that of measurements showing the three specific phases of MPB development during experimental conditions. Moreover, this 3rd test better simulated the amplitude of variation than the two previous simulations with almost the same standard deviation as observation, and displayed the lowest RMSE (~2) and the best correlation (R~0.98) among all simulations (Fig. 3, left graph red point).

3.2.2. Physiological thresholds triggering vertical migration

* Corresponding author: rakotomalala.c@gmail.com

Varying the threshold parameters triggering the downward (qC2N) and upward (qN2C) of diatom cells in the sediment led to different dynamics of MPB in the system, however the latency phase was systematically reproduced (Fig. 5).

Decreasing the value of the downward migration threshold (qC2N) resulted in MPB biomass lower than what was observed (Fig. 5, qC2N -30% and -50%). Moreover, the moderate and exponential growth were not reproduced depicted by lower SD value (~5 mol C m^{-3}) compared to the SD of observation and the reference (~12 mol C m^{-3}) (Supplementary Material SM2 Fig. 1 and 2). The extent of the carbon increment was more pronounced when the same threshold value was increased (Fig. 5, qC2N +30% and +50%) however the dynamics of MPB growth showed almost constant daily growth and again did not displayed the two last growth phases of MPB which was reflected by higher SD (between 20 and 25 mol C m^{-3}) regarding observed and reference simulation patterns (Supplementary Material SM2 Fig. 1 and 2).

* Corresponding author: rakotomalala.c@gmail.com

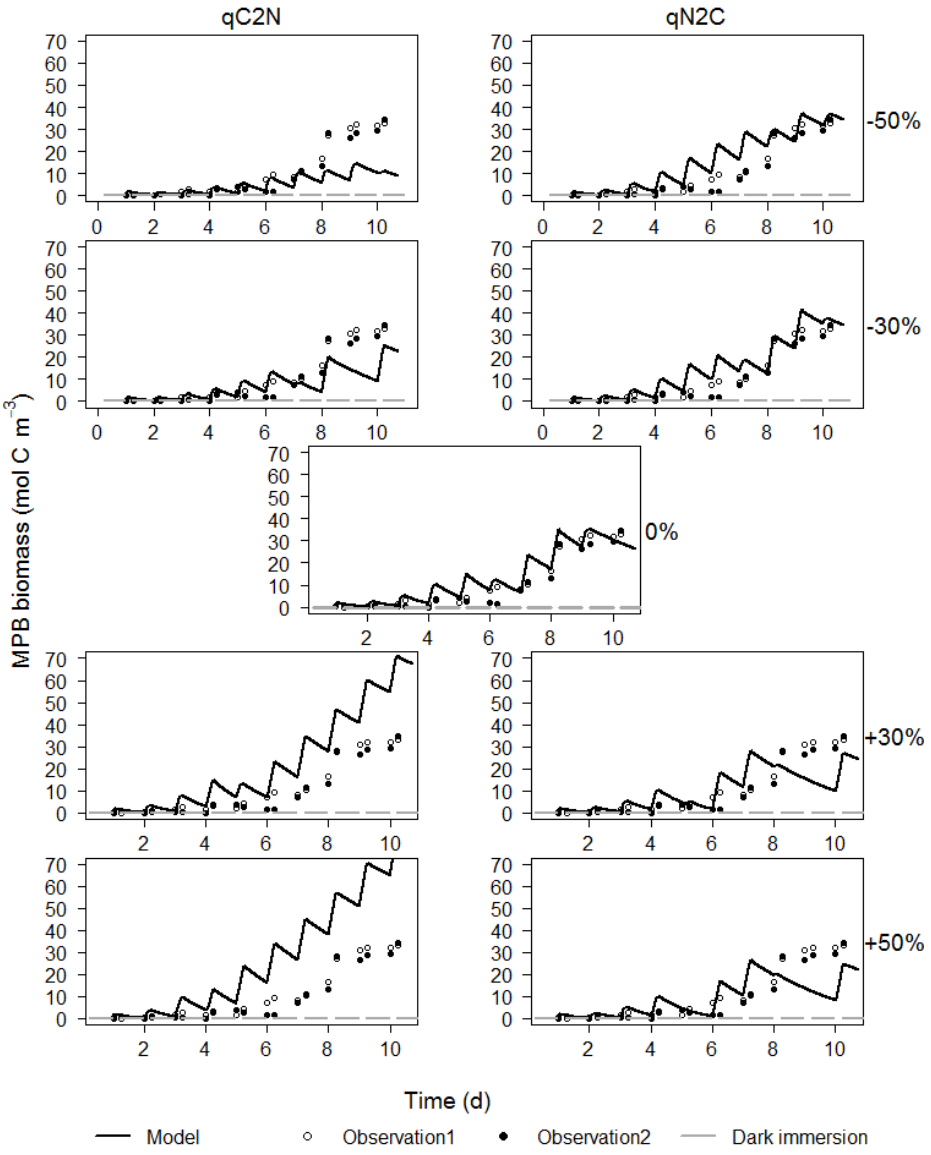

351

352 *Fig. 5: Simulations (lines) of diatom dynamics in the first centimeter of sediment obtained*
353 *while analyzing the sensitivity of the model by varying the qC2N and the qN2C by -50%, -30%,*
354 *0%, +30%, and +50% as 0% corresponds to best simulation with a biodiffusion 10 times higher*
355 *than the chemical diffusion. Measurements (points) were also represented on each graph. Gray*
356 *line represents dark immersion periods in the system.*

357 Earlier upward migration (lower values of qN2C) induced again daily photosynthetic
358 activity which slightly overestimated the simulation of reference as well as the observation (Fig.
359 5, qN2C -30% and -50%). However, simulations better fitted the observations mainly when the
360 threshold value was decreased by 30%, which showed almost the same SD as observation and
361 the simulation of reference and the lowest RMSE values (Supplementary Material SM2 Fig. 1
362 and 2). Simulated MPB biomass was characterized by cycles of high growth followed by 2 to

* Corresponding author: rakotomalala.c@gmail.com

3 days of decrease when upward migration was delayed (higher values of qN2C) (Fig.5 qN2C +30% and +50%). The patterns of these last simulations had the lowest correlation coefficient, low SD value and high RMSE compared to observation and the simulation of reference (Supplementary Material SM2 Fig. 1 and 2).

4. Discussion

4.1. Exogenous Vs endogenous factors controlling MPB vertical migration

A model of a benthic system which simulates physiological functioning of MPB, concomitant development of bacteria, and fluctuation of nutrients in the first centimeter of sediment was developed in this study. Simulations obtained from the model realistically reproduced the dynamics of MPB biomass measured in the first centimeter of sediment in laboratory experiments (Orvain et al., 2003). The model succeeded in reproducing the vertical migration of epipelic diatoms which follows the periodicity of tide and light as encountered in laboratory (Perkins et al., 2010) and also *in situ* (Blanchard et al., 2001). Cyclic simulated carbon assimilation during daytime emersion followed by carbon decrease during dark immersion regulated the upward and downward migration of cells between an active layer, where photosynthesis outcompeted respiration, and an inactive layer, where photosynthesis did not occur thus respiration dominated. The model was set up with the hypothesis that intra-cellular C/N quota determines the vertical migration of epipelic diatoms cells in the sediment together with tide and light. Debate is still open about the main factors driving the vertical migration of MPB in the sediment and this modelling approach offers some opportunities to discuss them. In their study, Consalvey et al. (2004) and Saburova and Polikarpov (2003) recapitulated factors that likely induce vertical migration of MPB which include exogenous and endogenous processes. Light was shown to be the "zeitgeber" (Mitbavkar and Anil, 2004) of the chronobiologic behavior, and especially the upward migration. However, Kingston (2002) has also showed that nutrients and carbon gradients at the surface could explain the downward migration of diatoms cells. Our results substantiate that exogenous factors (light and tide) and mainly endogenous factor (C/N ratio) control diatom migration. In densely packed biofilm, high competition for nutrients (Orvain et al., 2003) and increase of carbon content in MPB at the surface lead to an unbalanced C/N ratio in cells which migrate down to the sediment where higher availability of nutrients in reduced form is encountered (Magni and Montani, 2006), supporting the assumption of more favorable nutrient conditions at depth (Saburova and Polikarpov, 2003). In addition, accumulation of intracellular nutrient has been observed for benthic microalgae (Garcia-Robledo et al., 2016). Nutrient uptake at the surface and especially

* Corresponding author: rakotomalala.c@gmail.com

396 in the aphotic layer were well simulated since an increase of MPB nitrogen content occurred
397 mainly during dark immersion. Saburova and Polikarpov (2003) already illustrated decoupled
398 photosynthesis and cells division associated to high concentration of DIN in the sediment. Thus,
399 decoupled assimilations of C and N integrated in the model appeared to be realistic and could
400 reflect reality. Adjustment of the intracellular C/N gradient is thus achieved through vertical
401 migration which allowed efficient benthic microalgae functioning. The same patterns has been
402 observed with phytoplankton with varying C/N ratio during light period under N-sufficient
403 condition (Jauzein et al., 2011). The same decoupling of nitrogen and carbon assimilation has
404 also been reported for marine microalgae including diatoms (Clark and Flynn, 2002; Jauzein et
405 al., 2008; Schartau et al., 2007). Flynn and Fasham (2002) also suggested a link between
406 phytoplankton migration cycle and intercellular nitrogen content.
407 Choosing the carbon and the nitrogen requirements to predict vertical migration of epipelic
408 diatom represents new approach which in our knowledge has not been applied to benthic system
409 models yet. This may explain the decrease of the chl *a* concentration almost 2h before the end
410 of the light period (Cartaxana et al., 2016). The downward migration is thus highly driven by
411 endogenous processes in diatoms cells. Elemental requirements could also explain the
412 resuspension of MPB in the water column without sediment erosion encountered in the study
413 of Guarini et al. (2008) and what Mariotti and Fagherazzi (2012) designated as chronic
414 detachment. As long as N in the diatom cells is sufficient, MPB continues carbon photo-
415 assimilation even during rising tide. When the C/N ratio is unbalanced again with cells that are
416 in excess of N and the carbon stock is insufficient for respiration, the cells migrate back up to
417 the surface during low tide and daylight hours. This finding could also be the factor involved in
418 the presence of incipient diatom cells hours before ebb tide (Cartaxana et al., 2016) depicted as
419 the initial lag phase of MPB upward migration (Coelho et al., 2011).
420 In addition to vertical migration, photoprotection or even photoinhibition could be
421 encountered when MPB is subjected to high light (Cartaxana et al., 2011) and could explain a
422 downward migration before the end of the exposure low tide periods. Extreme temperature
423 clearly impairs microalgae growth and viability (Béchet et al., 2017), whose effect could be
424 synergetic with that of light (Laviale et al., 2015). Savelli et al. (2018) showed the relevant role
425 of the thermoinhibition on the summer primary production of MPB. However, as neither
426 temperature (~16°C) nor light intensity (120 µmol photons m^{-2}) during the mesocosm
427 experiment did not reach extreme values, the model is suited for experimental conditions.
428 However, it should be noted that MPB growth limited by temperature and light was already

* *Corresponding author: rakotomalala.c@gmail.com*

formulated in the model (Appendix Table 3). And compared to Guarini et al. (2000b), the value of optimum temperature were modified (20°C instead of 25°C) to better fit field data (unpublished data, Guizien K., Personal communication) in Marennes Olérons Bay during field survey (Orvain et al., 2014).

Sensitivity analysis conducted on the two threshold values of migration showed that they were sensitive and greatly determined the dynamics of MPB. Varying those values supposed either nitrogen or carbon assimilation is shorter or longer and resulted in different simulations. The effect of elemental requirements was hidden by chronobiological growth of MPB when cell were photosynthetically active longer at the surface and when cells migrated earlier at the surface (Fig. 5, qC2N+30%, qC2N +50%, qN2C-30%, and qN2C-50%). In contrast, when cells assimilated nitrogen longer in the sediment or when they migrated earlier down to the sediment, nitrogen assimilation lasted longer and was followed by important MPB growth, thus the effect of internal requirement overtook the chronobiological effect in MPB growth.

The internal C/N ratio of MPB then highly controls its dynamics in the sediment. The modeled C/N ratio in this study fluctuated between 1 and 3.5 with a constant PAR (140 µmol photons m^{-2} s^{-1}). In a different approach, Ross and Geider (2009) improved the initial model of Geider et al. (1998) which simulated total carbon and nitrogen contents of planktonic microalgae whose ratio oscillated between 5 to 6 and 7 to 13 with a forcing PAR of 60 and 1200 µmol photons m^{-2} s^{-1} respectively. The difference comes especially from the carbon simulated in Ross and Geider (2009) which represents the total carbon content whereas the carbon simulated herein represents only a part of the total carbon which is involved directly in the photosynthesis process leading to a C/N ratio value lower than in the literature.

This modeling exercise helped to explain processes on which questions remained open. However, the reproduction of the same growth dynamics of MPB during an experimental condition highlighted the importance of C/N ratio balance in its functioning. Further investigations of the fate of C/N ratios in epipelic diatoms cells and the empirically estimated C/N thresholds driving the vertical migration need to be conducted to improve the model robustness.

4.2.Bacteria, EPS, and MPB dynamics

Synergistic temporal variations of MPB, bacteria, and nutrients were required to obtain realistic reproduction of MPB growth observed during the experimental investigation by Orvain et al. (2003). The model succeeded in maintaining the three-phased growth of MPB. Moreover, decrease of bacterial biomass during daytime exposure was depicted while an important

* Corresponding author: rakotomalala.c@gmail.com

462 increase was observed during dark immersion. Orvain et al. (2014) observed in natural
463 condition a negative correlation between bound EPS exuded by MPB and bacteria in the
464 sediment only during growth phase. Such findings have been reiterated during experimental
465 investigations (Agogué et al., 2014; Doghri et al., 2017). The formulation of bacterial
466 development in the model integrated the inhibition effect of photosynthetic overflow DOC. This
467 negative correlation seemed to be more straightforward in these studies and this hypothesis
468 seemed to explain the observed alternating opposition of growth between bacteria (during
469 immersion nocturnal periods) and MPB (during daylight low-tide). However, positive effect of
470 bacteria on diatoms growth could also be encountered depending on species (Jauffrais et al.,
471 2017). Further analysis should be conducted to seek out the potential effect of bacteria on MPB
472 at the community level. Bacterial loss in marine system has been attributed to mortality through
473 viral lysis (Fischer et al., 2003; Tsai et al., 2013) which was the case in this study.
474 Competition between MPB and bacteria on nutrients was temporally delayed as bacteria
475 relied on DON while the MPB relied on DIN. The DON then fueled the DIN through bacterial
476 mineralization (Bohórquez et al., 2017) which could partly explain the opposed short-term
477 dynamics of bacteria and MPB. Risgaard-Petersen et al. (2004) found lower bacterial activity
478 in the presence of MPB attributed to direct competition on nutrients but could also be combined
479 with the previously mentioned inhibition effect of MPB on bacteria. As the same MPB growth
480 pattern was obtained during the experiment and with the model, interactions between bacteria
481 and MPB in the model appears realistic despite the absence of bacteria biomass measurement
482 during the study of Orvain et al. (2003). The inhibition effect of MPB on bacterial growth
483 appeared to encompass both complex interaction between them and their direct competition on
484 nutrients. However, formulation needs to be improved and validated, by refining the DIN
485 composition (ammonium, nitrates, nitrites...), by integrating the competition for ammonium
486 between MPB and bacteria, and by taking into account other processes related to the
487 regeneration of nutrients from organic matter as in Hochard et al. (2010).

488 **4.3. EPS nature Vs EPS function**

489 Diatoms DOC production was modelled based on their functions overflow release during
490 photosynthesis and should strictly corresponds to highly assimilable carbohydrates molecules.
491 Orvain et al. (2003) stated that the insoluble EPS (HMW) was more associated with the diatoms
492 and represented an overflow of carbon during photosynthesis in nutrient-depleted situation.
493 Moreover, photosynthesis is a processes involved in EPS production (Smith and Underwood,
494 2000; Staats et al., 2000). Both modelled EPS (DOC) and measured EPS HMW displayed daily

* *Corresponding author: rakotomalala.c@gmail.com*

fluctuation characterized by secretion during daytime exposure. Sudden drop was simulated during the successive dark immersion periods. Tidal and diel dynamics of EPS were in accordance with study of Agogué et al. (2014). Carbon exudation by MPB is associated with what Schartau et al. (2007) called carbon overconsumption or overflow metabolism (de Brouwer and Stal, 2001). The maximum overflow metabolism was simulated in day 8 before a downward migration of MPB in this study. They found that the first excretion happened during the growth phase while the second excretion took place under nutrient-depleted condition (Orvain et al., 2003). Other studies have also found higher production of EPS during the stationary phase (Agogué et al., 2014; Pierre et al., 2014; Staats et al., 2000). In our study, important photosynthesis-related EPS were modelled during strong growth with the maximum value the day 8, whereas the second mode happening during nutrient-depleted stationary phase was not maintained the two last days of simulation. Modified EPS extraction protocols (Takahashi et al., 2009) showed that colloidal fraction were glucose-rich probably because of a metabolic route related to photosynthesis. The latter could fit with the description of the photosynthetic related EPS modelled in this study. Colloidal EPS fractions were found to have biochemical composition related to carbon storage and were known to be a carbon source for heterotrophic bacteria (Cook et al., 2007; Pierre et al., 2014).

The second type of EPS was released during MPB migration as DON and as a loss of carbon outside the modelled system (Bohórquez et al., 2017). EPS compounds include a variety of molecules nature and weight some consisting of glycoproteins (Pierre et al., 2014). Orvain et al. (2003) described the LMW fraction as remnants of algal cells during movement. Moreover, Serôdio et al., (1997) recorded migratory pattern which was maintained when cultures were darkened. MPB cell must have internal reserves allowing them to synthesize EPS during a relative long period, even in absence of light. By the same token, Smith and Underwood (1998) mentioned the hypothesis of migration-specific EPS production by epipelic diatoms. “Cells locomotion requirement” in their study can be associated to C/N ratio modelled in this study and which forced the upward or the downward migration. Furthermore, our hypothesis of EPS produced while cells migrate within the sediment thus appears realistic. The presence of nitrogen in EPS were identified (Agogué et al., 2014; Pierre et al., 2014) supporting the expression in DON of the migration-related EPS in the model.

However, the differentiation of the EPS related to photosynthesis (carbon) and migration (nitrogen and carbon) in this study may not be roughly sketched since EPS production seems to be accompanied by high secretion of monomers (rhamnose, fucose, galactose, uronic acids …)

* Corresponding author: rakotomalala.c@gmail.com

as well as proteins (Agogué et al., 2014; Takahashi et al., 2009). Moreover, further analysis should be conducted to better account for the potential effect of varying salinity on EPS production. High tolerance to varying salinity was observed with an epipelic diatom species in controlled conditions where vertical migration was avoided (Juneau et al., 2015). However, stimulated EPS production was observed with high salinity in natural conditions (Orvain et al., 2014) which has protective role on MPB cells (Steele et al., 2014). The incorporation of the EPS secretion in the model implementation must be thus improved and better evaluated.

4.4. Importance of nutrient availability

MPB development was highly limited by nutrients. Daily variation of MPB concentration was mainly attributed to endogenous factors, however, nutrient depletion was the main factor driving the plateau phase of MPB dynamics. In our study, the diffusion of nutrients from the deeper layer was mandatory to reproduce the typical 3 phase growth pattern of MPB. High variability of the diffusivity coefficient in the sediment was reported in the literature (Li and Gregory, 1974). However, the chosen value in this study was of the same order of magnitude as the diffusivity coefficient often used in the literature (ca. 1.9×10^{-9} m^2 s^{-1}) (Bolałek and Graca, 1996). The dynamics of observed MPB biomass along the 10-day experiment were underestimated with chemical diffusion alone. Integration of nutrient availability, hypothesized to be enhanced by faunal activity, greatly ameliorated the quality of the simulations. The best simulation was obtained with a biodiffusion 10 fold higher than the chemical diffusion. Faunal induced diffusion of nutrients by the benthic fauna was important in our simulations especially when the nutrient concentration at the surface was low. The sensitivity analysis to biodiffusion highlighted that the lower the nutrient concentrations, the more important the biodiffusion. Faunal activities can indeed impact dissolved nutrient loads (Heilskov et al., 2006; Laverock et al., 2011) in a system which enhances primary productivity (Cadée, 1993; Chennu et al., 2015). As meiofauna (nematodes and foraminifera), was still observed in the experimental system (Orvain et al., 2003), nutrient supply could have resulted from processes such as bio-irrigation, nutrient release, and enhanced bacterial activity (Schratzberger and Ingels, 2018). Active bioturbator may create burrows in the sediment that enhance irrigation of solutes such as ammonium and nitrate (Aller and Aller, 1992; Christensen et al., 2000). Moreover, secretion of nutrients by meiofauna (D'Hondt et al., 2018) could also take place as found with macrofauna (Cadée, 1993; Gardner et al., 2006). Hence, integrating the bio-irrigation related to the meiofauna activities, as conducted by Butenschön et al. (2016), should be performed to better analyze the biogeochemical functioning of estuarine benthic systems.

* *Corresponding author: rakotomalala.c@gmail.com*

The model developed herein is suited to reproduce development of MPB in controlled conditions. The model could also be directly used to analyze benthic system functioning in natural conditions only if all influencing compartments were taken into account. Indeed, MPB consumption by macrofauna and nutrient availability due to faunal activity was required when the model was used to analyze the functioning of Marennes-Oléron (France) mudflat and which gave satisfactory dynamics of the MPB compared to measurements (unpublished data, Guizien K., Personal communication). Moreover, *in situ* application of the model will require accurate tidal and light cycles. Light attenuation in the water column should be taken into account for low turbidity zone such as subtidal system, while hypothesizing development of MPB during diurnal low tide could reflect natural condition of a system with high turbidity of the water column, encountered in most of intertidal mudflats.

5. Conclusion

A model was developed in this study which simulates the functioning of a biogeochemical benthic system constituted of MPB and associated EPS release, bacteria, and nutrients. Simulations highlighted that MPB dynamics was highly limited by nutrient availability in the surficial sediment. Observed three-phased MPB dynamics was only reproduced by integrating an enhanced nutrient flux attributed to meiofauna activity. Moreover, this study figures among the first attempts in integrating EPS production, MPB and bacterial development in a benthic system model. The model also used a new approach by taking into account the carbon and nitrogen requirements as major drivers in vertical migration of MPB. This was made possible by decoupling carbon and nitrogen metabolisms. Formulation of MPB functioning in this study will improve integration of MPB into biogeochemical models, such as in the study of Hochard et al. (2010), to better analyze the functioning of benthic estuarine ecosystems.

Acknowledgments

This work was conducted as part of VASIREMI project (2006-2010) funded by "Agence Nationale de la Recherche" and as part of doctoral research project funded by "Agence de l'Eau Seine Normandie" and "Région Basse Normandie" (2012-2016). Our special thanks to Jean-Marc Guarini, Frédéric Diaz, and Charlotte Moritz for their valuable contribution to this work. We warmly thank the three reviewers for their constructive comments.

* *Corresponding author: rakotomalala.c@gmail.com*

Literature cited

Agogué, H., Mallet, C., Orvain, F., De Crignis, M., Mornet, F., Dupuy, C., 2014. Bacterial dynamics in a microphytobenthic biofilm: A tidal mesocosm approach. J. Sea Res. 92, 36–45. https://doi.org/10.1016/j.seares.2014.03.003

Aller, R.C., Aller, J.Y., 1992. Meiofauna and solute transport in marine muds. Limnol. Oceanogr. 37, 1018–1033. https://doi.org/10.4319/lo.1992.37.5.1018

Baklouti, M., Faure, V., Pawlowski, L., Sciandra, A., 2006. Investigation and sensitivity analysis of a mechanistic phytoplankton model implemented in a new modular numerical tool (Eco3M) dedicated to biogeochemical modelling. Prog. Oceanogr. 71, 34–58. https://doi.org/10.1016/j.pocean.2006.05.003

Barnett, A., Méléder, V., Blommaert, L., Lepetit, B., Gaudin, P., Vyverman, W., Sabbe, K., Dupuy, C., Lavaud, J., 2015. Growth form defines physiological photoprotective capacity in intertidal benthic diatoms. Int. Soc. Microb. Ecol. 32–45. https://doi.org/10.1038/ismej.2014.105

Barranguet, C., Plante-Cuny, M.R., Alivon, E., 1996. Microphytobenthos production in the Gulf of Fos, French Mediterranean coast. Hydrobiologia 333, 181–193. https://doi.org/10.1007/BF00013432

Béchet, Q., Laviale, M., Arsapin, N., Bonnefond, H., Bernard, O., 2017. Modeling the impact of high temperatures on microalgal viability and photosynthetic activity. Biotechnol. Biofuels 10, pp.136. https://doi.org/10.1186/s13068-017-0823-z

Bernard, O., 2011. Hurdles and challenges for modelling and control of microalgae for CO2 mitigation and biofuel production. J. Process Control 21, 1378–1389. https://doi.org/10.1016/j.jprocont.2011.07.012

Blackford, J.C., 2002. The influence of microphytobenthos on the Northern Adriatic ecosystem: A modelling study. Estuar. Coast. Shelf Sci. 55, 109–123. https://doi.org/10.1006/ecss.2001.0890

Blanchard, G.F., Guarini, J.-M., Orvain, F., Sauriau, P.-G., 2001. Dynamic behaviour of benthic microalgal biomass in intertidal mudflats. J. Exp. Mar. Bio. Ecol. 264, 85–100. https://doi.org/10.1016/S0022-0981(01)00312-4

Blanchard, G.F., Guarini, J.-M., Richard, P., Gros, P., Mornet, F., 1996. Quantifying the short-term temperature effect in light-saturated photosynthesis of intertidal microphytobenthos. Mar. Ecol. Prog. 134, 309–313. https://doi.org/doi:10.3354/meps134309

Bohórquez, J., McGenity, T.J., Papaspyrou, S., García-Robledo, E., Corzo, A., Underwood,

* *Corresponding author: rakotomalala.c@gmail.com*

G.J.C., 2017. Different types of diatom-derived extracellular polymeric substances drive changes in heterotrophic bacterial communities from intertidal sediments. Front. Microbiol. 8:245. https://doi.org/10.3389/fmicb.2017.00245

Bolałek, J., Graca, B., 1996. Ammonia Nitrogen at the Water–Sediment Interface in Puck Bay (Baltic Sea). Estuar. Coast. Shelf Sci. 43, 767–779. https://doi.org/10.1006/ecss.1996.0102

Boudreau, B.P., 1996. The diffusive tortuosity of fine-grained unlithified sediments. Geochim. Cosmochim. Acta 60, 3139–3142. https://doi.org/10.1016/0016-7037(96)00158-5

Butenschön, M., Clark, J., Aldridge, J.N., Allen, J.I., Artioli, Y., Blackford, J., Bruggeman, J., Cazenave, P., Ciavatta, S., Kay, S., Lessin, G., van Leeuwen, S., van der Molen, J., de Mora, L., Polimene, L., Sailley, S., Stephens, N., Torres, R., 2016. ERSEM 15.06 : a generic model for marine biogeochemistry and the ecosystem dynamics of the lower trophic levels. Geosci. Model Dev. 9, 1293–1339. https://doi.org/10.5194/gmd-9-1293-2016

Cadée, N., 1993. The uptake and release of material by the cockle *Cerastoderma edule L.* in the Western Scheldt Estuary, SW Netherlands. Natl. Inst. Coast. Mar. Manag. /RIKZ Middelburg, Netherlands.

Cartaxana, P., Cruz, S., Gameiro, C., Kühl, M., 2016. Regulation of intertidal microphytobenthos photosynthesis over a diel emersion period is strongly affected by diatom migration patterns. Front. Microbiol. 7, 1–11. https://doi.org/10.3389/fmicb.2016.00872

Cartaxana, P., Ruivo, M., Hubas, C., Davidson, I., Serôdio, J., Jesus, B., 2011. Physiological versus behavioral photoprotection in intertidal epipelic and epipsammic benthic diatom communities. J. Exp. Mar. Bio. Ecol. 405, 120–127. https://doi.org/10.1016/j.jembe.2011.05.027

Chennu, A., Volkenborn, N., De Beer, D., Wethey, D.S., Woodin, S.A., Polerecky, L., 2015. Effects of bioadvection by *Arenicola marina* on microphytobenthos in permeable sediments. PLoS One 10, 1–16. https://doi.org/10.1371/journal.pone.0134236

Christensen, B., Vedel, A., Kristensen, E., 2000. Carbon and nitrogen fluxes in sediment inhabited by suspension-feeding (*Nereis diversicolor*) and non-suspension-feeding (*N. virens*) polychaetes. Mar. Ecol. Prog. Ser. 192, 203–217. https://doi.org/10.3354/meps192203

Clark, D.R., Flynn, K.J., 2002. N-assimilation in the noxious flagellate *Heterosigma carterae* (Raphidophyceae): Dependence on light, N-source, and physiological state. J. Phycol. 38,

* *Corresponding author: rakotomalala.c@gmail.com*

503–512. https://doi.org/10.1046/j.1529-8817.2002.t01-1-01082.x

Cloern, J.E., Foster, S.Q., Kleckner, A.E., 2014. Phytoplankton primary production in the world's estuarine-coastal ecosystems. Biogeosciences 11, 2477–2501. https://doi.org/10.5194/bg-11-2477-2014

Coelho, H., Vieira, S., Serôdio, J., Nia Vieira Ã, S., Ser Dio, J.O., 2011. Endogenous versus environmental control of vertical migration by intertidal benthic microalgae. Eur. J. Phycol. Eur. J. Phycol 463, 271–281. https://doi.org/10.1080/09670262.2011.598242

Consalvey, M., Paterson, M.D., Underwood, G.J.C., 2004. The Ups and Downs of Life in a Benthic Biofilm : Migration of Benthic Diatoms. Diatom Res. 19, 181–202. https://doi.org/10.1080/0269249X.2004.9705870

Cook, P.L.M., Veuger, B., Böeer, S., Middelburg, J.J., 2007. Effect of nutrient availability on carbon and nitrogen incorporation and flows through benthic algae and bacteria in near-shore sandy sediment. Aquat. Microb. Ecol. 49, 165–180. https://doi.org/10.3354/ame01142

D'Hondt, A.S., Stock, W., Blommaert, L., Moens, T., Sabbe, K., 2018. Nematodes stimulate biomass accumulation in a multispecies diatom biofilm. Mar. Environ. Res. 140, 78–89. https://doi.org/10.1016/j.marenvres.2018.06.005

de Brouwer, J.F.C., Neu, T.R., Stal, L.J., 2006. On the function of secretion of extracellular polymeric substances by benthic diatoms and their role in intertidal mudflats: A review of recent insights and views, in: Kromkamp, J.C., Brouwer, J.F.C. De, Blanchard, G.F., Forster, R.M., Créach, V. (Eds.), Functioning of Microphytobenthos in Estuaries : Proceedings of the Colloquium, Amsterdam, 21-23 August 2003. Royal Netherlands Academy of Arts and Sciences, Amsterdam, pp. 45–61. https://doi.org/10.1086/586980

de Brouwer, J.F.C., Stal, L.J., 2001. Short-term dynamics in microphytobenthos distribution and associated extracellular carbohydrates in surface sediments of an intertidal mudflat. Mar. Ecol. Prog. Ser. 218, 33–44. https://doi.org/10.3354/meps218033

de Jonge, V.N., Van Beusekom, J.E.E., 1992. Contribution of resuspended microphytobenthos to total phytoplankton in the EMS estuary and its possible role for grazers. Netherlands J. Sea Res. 30, 91–105. https://doi.org/10.1016/0077-7579(92)90049-K

Doghri, I., Lavaud, J., Dufour, A., Bazire, A., Lanneluc, I., Sablé, S., 2017. Cell-bound exopolysaccharides from an axenic culture of the intertidal mudflat Navicula phyllepta diatom affect biofilm formation by benthic bacteria. J. Appl. Phycol. 29, 165–177. https://doi.org/10.1007/s10811-016-0943-z

* *Corresponding author: rakotomalala.c@gmail.com*

693 Fischer, U.R., Wieltschnig, C., Kirschner, A.K.T., Velimirov, B., 2003. Does virus-induced
694 lysis contribute significantly to bacterial mortality in the oxygenated sediment layer of
695 shallow oxbow lakes? Appl. Environ. Microbiol. 69, 5281–5289.
696 https://doi.org/10.1128/AEM.69.9.5281-5289.2003
697 Flynn, K.J., Fasham, M.J.R., 2002. A modelling exploration of vertical migration by
698 phytoplankton. J. Theor. Biol. 218, 471–484. https://doi.org/10.1006/yjtbi.3093
699 Garcia-Robledo, E., Bohorquez, J., Corzo, A., Jimenez-Arias, J.L., Papaspyrou, S., 2016.
700 Dynamics of Inorganic Nutrients in Intertidal Sediments : Porewater , Exchangeable , and
701 Intracellular Pools. Front. Microbiol. 7, 1–14. https://doi.org/10.3389/fmicb.2016.00761
702 Gardner, W.S., Briones, E.E., Kaegi, E.C., Rowe, G.T., 2006. Ammonium Excretion by Benthic
703 Invertebrates and Sediment-Water Nitrogen Flux in the Gulf of Mexico near the
704 Mississippi River Outflow. Estuaries 16, 799. https://doi.org/10.2307/1352438
705 Gaudron, S.M., Grangeré, K., Lefebvre, S., 2016. The Comparison of δ13C Values of a Deposit-
706 and a Suspension-Feeder Bio-Indicates Benthic vs. Pelagic Couplings and Trophic Status
707 in Contrasted Coastal Ecosystems. Estuaries and Coasts 39, 731–741.
708 https://doi.org/10.1007/s12237-015-0020-x
709 Geider, R., MacIntyre, H.L., Kana, T.M., 1998. A dynamic regulatory model of
710 phytoplanktonic acclimation to light, nutrients and temperature. Limnol. Oceanogr. 43,
711 679–694. https://doi.org/10.4319/lo.1998.43.4.0679
712 Guarini, J.-M., Blanchard, G.F., Gros, P., 2000a. Quantification of the microphytobenthic
713 primary production in european intertidal mudflats - A modelling approach. Cont. Shelf
714 Res. 20, 1771–1788. https://doi.org/10.1016/S0278-4343(00)00047-9
715 Guarini, J.-M., Blanchard, G.F., Gros, P., Gouleau, D., Bacher, C., 2000b. Dynamic model of
716 the short-term variability of microphytobenthic biomass on temperate intertidal mudflats.
717 Mar. Ecol. Prog. Ser. 195, 291–303. https://doi.org/10.3354/meps195291
718 Guarini, J.-M., Sari, N., Moritz, C., 2008. Modelling the dynamics of the microalgal biomass
719 in semi-enclosed shallow-water ecosystems. Ecol. Modell. 211, 267–278.
720 https://doi.org/10.1016/j.ecolmodel.2007.09.011
721 Heilskov, A.C., Alperin, M., Holmer, M., 2006. Benthic fauna bio-irrigation effects on nutrient
722 regeneration in fish farm sediments. J. Exp. Mar. Bio. Ecol. 339, 204–225.
723 https://doi.org/10.1016/j.jembe.2006.08.003
724 Hochard, S., Pinazo, C., Grenz, C., Evans, J.L.B., Pringault, O., 2010. Impact of
725 microphytobenthos on the sediment biogeochemical cycles: A modeling approach. Ecol.

* *Corresponding author: rakotomalala.c@gmail.com*

726 Modell. 221, 1687–1701. https://doi.org/10.1016/j.ecolmodel.2010.04.002
727 Hochard, S., Pinazo, C., Rochelle-newall, E., Pringault, O., 2012. Benthic pelagic coupling in
728 a shallow oligotrophic ecosystem : Importance of microphytobenthos and physical forcing.
729 Ecol. Modell. 247, 307–318. https://doi.org/10.1016/j.ecolmodel.2012.07.038
730 Jauffrais, T., Agogué, H., Gemin, M.P., Beaugeard, L., Martin-Jézéquel, V., 2017. Effect of
731 bacteria on growth and biochemical composition of two benthic diatoms *Halamphora*
732 *coffeaeformis* and *Entomoneis paludosa*. J. Exp. Mar. Bio. Ecol. 495, 65–74.
733 https://doi.org/10.1016/j.jembe.2017.06.004
734 Jauzein, C., Collos, Y., Garcés, E., Vila, M., Maso, M., 2008. Short-term temporal variability
735 of ammonium and urea uptake by *Alexandrium catenella* (Dinophyta) in cultures. J.
736 Phycol. 44, 1136–1145. https://doi.org/10.1111/j.1529-8817.2008.00570.x
737 Jauzein, C., Collos, Y., Laabir, M., Vaquer, A., 2011. Dark metabolism and carbon-nitrogen
738 uncoupling in the toxic dinoflagellate *Alexandrium catenella* (Dinophyceae). Harmful
739 Algae 11, 73–80. https://doi.org/10.1016/j.hal.2011.08.002
740 Juneau, P., Barnett, A., Méléder, V., Dupuy, C., Lavaud, J., 2015. Combined effect of high light
741 and high salinity on the regulation of photosynthesis in three diatom species belonging to
742 the main growth forms of intertidal flat inhabiting microphytobenthos. J. Exp. Mar. Bio.
743 Ecol. 463, 95–104. https://doi.org/10.1016/j.jembe.2014.11.003
744 Kang, C.K., Park, H.J., Choy, E.J., Choi, K.S., Hwang, K., Kim, J. Bin, 2015. Linking intertidal
745 and subtidal food webs: Consumer-mediated transport of intertidal benthic microalgal
746 carbon. PLoS One 10. https://doi.org/10.1371/journal.pone.0139802
747 Kingston, M.B., 2002. Effect of subsurface nutrient supplies on the vertical migration of
748 *Euglena proxima* (Euglenophyta). J. Phycol. 38, 872–880. https://doi.org/10.1046/j.1529-
749 8817.2002.t01-1-01197.x
750 Kromkamp, J., Barranguet, C., Peene, J., 1998. Determination of microphytobenthos PSII
751 quantum efficiency and photosynthetic activity by means of variable chlorophyll
752 fluorescence. Mar. Ecol. Prog. Ser. 162, 45–55. https://doi.org/10.3354/meps162045
753 Laverock, B., Gilbert, J. a, Tait, K., Osborn, a M., Widdicombe, S., 2011. Bioturbation: impact
754 on the marine nitrogen cycle. Biochem. Soc. Trans. 39, 315–320.
755 https://doi.org/10.1042/BST0390315
756 Lavery, P.S., Oldham, C.E., Ghisalberti, M., 2001. The use of fick's first law for predicting
757 porewater nutrient fluxes under diffusive conditions. Hydrol. Process. 15, 2435–2451.
758 https://doi.org/10.1002/hyp.297

* *Corresponding author: rakotomalala.c@gmail.com*

759 Laviale, M., Barnett, A., Ezequiel, J., Lepetit, B., Frankenbach, S., Méléder, V., Serôdio, J.,
760 Lavaud, J., 2015. Response of intertidal benthic microalgal biofilms to a coupled light-
761 temperature stress: evidence for latitudinal adaptation along the Atlantic coast of Southern
762 Europe. Environ. Microbiol. 17, 3662–3677. https://doi.org/10.1111/1462-2920.12728
763 Le Chevanton, M., Garnier, M., Bougaran, G., Schreiber, N., Lukomska, E., Bérard, J.B.,
764 Fouilland, E., Bernard, O., Cadoret, J.P., 2013. Screening and selection of growth-
765 promoting bacteria for *Dunaliella* cultures. Algal Res. 2, 212–222.
766 https://doi.org/10.1016/j.algal.2013.05.003
767 Li, Y.-H., Gregory, S., 1974. Diffusion of ions in sea water and in deep sea sediment. Geochim.
768 Cosmochim. Acta 38, 703–714. https://doi.org/https://doi.org/10.1016/0016-
769 7037(74)90145-8
770 Magni, P., Montani, S., 2006. Seasonal patterns of pore-water nutrients, benthic chlorophyll *a*
771 and sedimentary AVS in a macrobenthos-rich tidal flat. Hydrobiologia 571, 297–311.
772 https://doi.org/10.1007/s10750-006-0242-9
773 Mariotti, G., Fagherazzi, S., 2012. Modeling the effect of tides and waves on benthic biofilms.
774 J. Geophys. Res. 117. https://doi.org/10.1029/2012JG002064
775 McKew, B.A., Taylor, J.D., McGenity, T.J., Underwood, G.J.C., 2011. Resistance and
776 resilience of benthic biofilm communities from a temperate saltmarsh to desiccation and
777 rewetting. ISME J. 5, 30–41. https://doi.org/10.1038/ismej.2010.91
778 Mitbavkar, S., Anil, a. C., 2004. Vertical migratory rhythms of benthic diatoms in a tropical
779 intertidal sand flat: influence of irradiance and tides. Mar. Biol. 145, 9–20.
780 https://doi.org/10.1007/s00227-004-1300-3
781 Ní Longphuirt, S., Lim, J.H., Leynaert, A., Claquin, P., Choy, E.J., Kang, C.K., An, S., 2009.
782 Dissolved inorganic nitrogen uptake by intertidal microphytobenthos: Nutrient
783 concentrations, light availability and migration. Mar. Ecol. Prog. Ser. 379, 33–44.
784 https://doi.org/10.3354/meps07852
785 Orvain, F., De Crignis, M., Guizien, K., Lefebvre, S., Mallet, C., Takahashi, E., Dupuy, C.,
786 2014. Tidal and seasonal effects on the short-term temporal patterns of bacteria,
787 microphytobenthos and exopolymers in natural intertidal biofilms (Brouage, France). J.
788 Sea Res. 92, 6–18. https://doi.org/10.1016/j.seares.2014.02.018
789 Orvain, F., Galois, R., Barnard, C., Sylvestre, A., Blanchard, G., Sauriau, P.G., 2003.
790 Carbohydrate production in relation to microphytobenthic biofilm development: An
791 integrated approach in a tidal mesocosm. Microb. Ecol. 45, 237–251.

* *Corresponding author: rakotomalala.c@gmail.com*

https://doi.org/10.1007/s00248-002-2027-7
Perkins, R.G., Lavaud, J., Serôdio, J., Mouget, J.L., Cartaxana, P., Rosa, P., Barille, L., Brotas, V., Jesus, B.M., 2010. Vertical cell movement is a primary response of intertidal benthic biofilms to increasing light dose. Mar. Ecol. Prog. Ser. 416, 93–103. https://doi.org/10.3354/meps08787
Pierre, G., Zhao, J.M., Orvain, F., Dupuy, C., Klein, G.L., Graber, M., Maugard, T., 2014. Seasonal dynamics of extracellular polymeric substances (EPS) in surface sediments of a diatom-dominated intertidal mudflat (Marennes-Oléron, France). J. Sea Res. 92, 26–35. https://doi.org/10.1016/j.seares.2013.07.018
Pinckney, J.L., Zingmark, R.G., 1993. Modelling the annual production of intertidal benthic microalgae in estuarine ecosystems. J. Phycol. 29, 396–407. https://doi.org/DOI 10.1111/j.1529-8817.1993.tb00140.x
Risgaard-Petersen, N., Nicolaisen, M.H., Revsbech, N.P., Lomstein, B.A., 2004. Competition between Ammonia-Oxidizing Bacteria and Benthic Microalgae. Appl. Environ. Microbiol. 70, 5528–5537. https://doi.org/10.1128/AEM.70.9.5528
Ross, O.N., Geider, R.J., 2009. New cell-based model of photosynthesis and photo-acclimation: accumulation and mobilisation of energy reserves in phytoplankton. Mar. Ecol. Prog. Ser. 383, 53–71. https://doi.org/10.3354/meps07961
Saburova, M.A., Polikarpov, I.G., 2003. Diatom activity within soft sediments: Behavioural and physiological processes. Mar. Ecol. Prog. Ser. 251, 115–126. https://doi.org/10.3354/meps251115
Savelli, R., Dupuy, C., Barillé, L., Lerouxel, A., Guizien, K., Philippe, A., Bocher, P., Polsenaere, P., Le Fouest, V., 2018. On biotic and abiotic drivers of the microphytobenthos seasonal cycle in a temperate intertidal mudflat: a modelling study. Biogeosciences 15, 7243–7271. https://doi.org/10.5194/bg-15-7243-2018
Schartau, M., Engel, A., Schröter, J., Thoms, S., Völker, C., Wolf-Gladrow, D., 2007. Modelling carbon overconsumption and the formation of extracellular particulate organic carbon. Biogeosciences 4, 433–454. https://doi.org/https://doi.org/10.5194/bg-4-433-2007
Schratzberger, M., Ingels, J., 2018. Meiofauna matters: The roles of meiofauna in benthic ecosystems. J. Exp. Mar. Bio. Ecol. 502, 12–25. https://doi.org/10.1016/j.jembe.2017.01.007
Serôdio, J., Catarino, F., 2000. Modelling the primary productivity of intertidal microphytobenthos: Time scales of variability and effects of migratory rhythms. Mar.

* *Corresponding author: rakotomalala.c@gmail.com*

825 Ecol. Prog. Ser. 192, 13–30. https://doi.org/10.3354/meps192013
826 Serôdio, J., Marques da Silva, J., Catarino, F., 1997. Nondestructive tracing of migratory
827 rhythms of intertidal benthic microalgae using in vivo chlorophyll *a* fluorescence. J.
828 Phycol. 553, 542–553. https://doi.org/DOI 10.1111/j.0022-3646.1997.00542.x
829 Shimoda, Y., Arhonditsis, G.B., 2016. Phytoplankton functional type modelling: Running
830 before we can walk? A critical evaluation of the current state of knowledge. Ecol. Modell.
831 320, 29–43. https://doi.org/10.1016/j.ecolmodel.2015.08.029
832 Siem-Jørgensen, M., Glud, R.N., Middelboe, M., 2008. Viral dynamics in a coastal sediment:
833 Seasonal pattern, controlling factors and relations to the pelagic-benthic coupling. Mar.
834 Biol. Res. 4, 165–179. https://doi.org/10.1080/17451000801888718
835 Smith, D.J., Underwood, G.J.C., 2000. The production of extracellular carbohydrates by
836 estaurine benthic diatoms: The effects of growth phase and light and dark treatment. J.
837 Phycol. 36, 321–333. https://doi.org/10.1046/j.1529-8817.2000.99148.x
838 Smith, D.J., Underwood, G.J.C., 1998. Exopolymer production by intertidal epipelic diatoms.
839 Limnol. Oceanogr. 43, 1578–1591. https://doi.org/10.4319/lo.1998.43.7.1578
840 Staats, N., Stal, L.J., de Winder, B., Mur, L.R., 2000. Oxygenic photosynthesis as driving
841 process in exopolysaccharide production of benthic diatoms. Mar. Ecol. Prog. Ser. 193,
842 261–269. https://doi.org/http://dx.doi.org/10.3354/meps193261
843 Steele, D.J., Franklin, D.J., Underwood, G.J.C., 2014. Protection of cells from salinity stress by
844 extracellular polymeric substances in diatom biofilms. Biofouling 30, 987–998.
845 https://doi.org/10.1080/08927014.2014.960859
846 Swanberg, L.I., 1991. The influence of the filter-feeding bivalve *Cerastoderma edule L.* on
847 microphytobenthos: a laboratory study. J. Exp. Mar. Bio. Ecol. 151, 93–111.
848 https://doi.org/10.1016/0022-0981(91)90018-R
849 Takahashi, E., Ledauphin, J., Goux, D., Orvain, F., 2009. Optimising extraction of extracellular
850 polymeric substances (EPS) from benthic diatoms: comparison of the efficiency of six EPS
851 extraction methods. Mar. Freshw. Res. 60, 1201–1210.
852 https://doi.org/http://dx.doi.org/10.1071/MF08258
853 Taylor, K.E., 2001. Summarizing multiple aspects of model performance in a single diagram.
854 J. Geophys. Res. 106, 7183–7192. https://doi.org/10.1029/2000JD900719
855 Tsai, a. Y., Gong, G.-C., Hung, J., 2013. Seasonal variations of virus- and nanoflagellate-
856 mediated mortality of heterotrophic bacteria in the coastal ecosystem of subtropical
857 western Pacific. Biogeosciences 10, 3055–3065. https://doi.org/10.5194/bg-10-3055-2013

* *Corresponding author: rakotomalala.c@gmail.com*

Ubertini, M., Lefebvre, S., Rakotomalala, C., Orvain, F., 2015. Impact of sediment grain-size and biofilm age on epipelic microphytobenthos resuspension. J. Exp. Mar. Bio. Ecol. 467, 52–64. https://doi.org/10.1016/j.jembe.2015.02.007

Underwood, G.J.C., Kromkamp, J., 1999. Primary Production by Phytoplankton and Microphytobenthos in Estuaries, in: Nedwell, D., Rafaell, D. (Eds.), Advances in Ecological Research Estuaries. Academic Press, San Diego, pp. 93–153.

Underwood, G.J.C., Paterson, D.M., 1993. Seasonal changes in diatom biomass, sediment stability and biogenic stabilization in the Severn Estuary. J. Mar. Biol. Assoc. United Kingdom 73, 871–887. https://doi.org/10.1017/S0025315400034780

Contribution of all authors

1- C.R., F.O., K.G., S.L., and C.D. conceived and designed the study.
2- The initial biogeochemical model with MPB and the secretion of EPS was conceived and designed by K.G., S.L., and F.O.
3- The coupling between EPS and bacteria was formulated by the 3 initial model conceptors and C.D.
4- The model development and parameterization was performed by C.R., K.G., F.O., S.L. and K.G.
5- All authors contributed to writing, reviewing and editing of the paper

Competing interest: The authors declare that they have no conflict of interest.

* Corresponding author: rakotomalala.c@gmail.com

Appendix

Table 1: Dependents: each pool is an average over the 1 cm of sediment

Dependent name	***Dependent meaning***	***Unit***
	State variables	
[Dact : C]	Energetic carbon pool in active diatom i.e. at mud surface	mol C m^{-3}
[Dact : N]	Nitrogen pool in active diatoms i.e. at mud surface	mol N m^{-3}
[D : C]	Energetic carbon pool in inactive diatoms i.e. below the mud surface	mol C m^{-3}
[D : N]	Nitrogen pool in inactive diatoms i.e. below the mud surface	mol N m^{-3}
[PON]	Particulate organic nitrogen pool	mol N m^{-3}
[DOC]	Dissolved organic carbon pool	mol C m^{-3}
[DON]	Dissolved organic nitrogen pool	mol N m^{-3}
[DIN]	Dissolved inorganic nitrogen pool	mol N m^{-3}
[Bact : N]	Nitrogen pool in bacteria	mol N m^{-3}
	Forcing variables	
E_{PAR}	Light intensity	W m^{-2}
T	Mud surface temperature	°C
h	Tide detection [0,1]	-
DIN_{sed}	Dissolved inorganic nitrogen pool over the 2nd cm depth	mol N m^{-3}

* Corresponding author: rakotomalala.c@gmail.com

903 Table 2: Model equations

$$\frac{d[Dact:C]}{dt} = \varphi(\infty,[Dact:C]) - \varphi([Dact:C],[D:C]) + \varphi([D:C],[Dact:C]) - \varphi([Dact:C],\infty)_E - \varphi([Dact:C],\infty)_R - \varphi(\infty,[DOC]) \quad (1)$$

$$\frac{d[Dact:N]}{dt} = \varphi([DIN],[Dact:N]) - \varphi([Dact:N],[D:N]) + \varphi([D:N],[Dact:N]) - \varphi([Dact:N],[DON]) \quad (2)$$

$$\frac{d[D:C]}{dt} = \varphi([Dact:C],[D:C]) - \varphi([D:C],[Dact:C]) - \varphi([D:C],\infty)_E - \varphi([D:C],\infty)_R - \varphi([D:C],\infty)_M \quad (3)$$

$$\frac{d[D:N]}{dt} = \varphi([DIN],[D:N]) + \varphi([Dact:N],[D:N]) - \varphi([D:N],[Dact:N]) - \varphi([D:N],[DON]) - \varphi([D:N],[PON]) \quad (4)$$

$$\frac{d[PON]}{dt} = \varphi([D:N],[PON]) - \varphi([PON],[DON]) \quad (5)$$

$$\frac{d[DOC]}{dt} = \varphi(\infty,[DOC]) - \varphi([DOC],\infty)_S \quad (6)$$

$$\frac{d[DON]}{dt} = \varphi([Dact:N],[DON]) + \varphi([D:N],[DON]) - \varphi([DON],[Bact:N]) + \varphi([Bact:N],[DON]) + \varphi([PON],[DON]) - \varphi([DON],[DIN]) \quad (7)$$

$$\frac{d[DIN]}{dt} = +\varphi([DON],[DIN]) + \varphi(\infty,[DIN]) - \varphi([DIN],[D:N]) - \varphi([DIN],[Dact:N]) \quad (8)$$

$$\frac{d[Bact:N]}{dt} = \varphi([DON],[Bact:N]) - \varphi([Bact:N],[DON]) \quad (9)$$

904

905 $\varphi([X],[Y])$ represents the flux transfer from compartment [X] to compartments [Y]

906 $\varphi([X],\infty)$ represents the flux lost from compartment [X]

907 $\varphi(\infty,[X])$ represents the flux input to compartment [X]

* Corresponding author: rakotomalala.c@gmail.com

Table 3: Specific functions for light and temperature limitation used in the model equations

$L_L = tanh\left(\frac{E_{PAR}}{K_{PAR}}\right)$	Light limitation
$L_T = \left(\frac{T_{max} - T}{T_{max} - T_{opt}}\right)^{\beta} e^{\left[-\beta\left(\frac{T_{max}-T}{T_{max}-T_{opt}}-1\right)\right]}$	Temperature limitation (Blanchard et al., 1996)

* Corresponding author: rakotomalala.c@gmail.com

933 Table 4: Model fluxes formulations

photosynthesis	$\varphi(\infty,[Dact:C]) = P_{max}\frac{[Dact:N]}{[Dact:N]+K_1}L_L L_T$	Inorganic carbon assimilation fueling epipelic diatoms energetic carbon pool as a result of photosynthesis
exu_photo	$\varphi(\infty,[DOC]) = \gamma_p \varphi(\infty,[Dact:C])$	Sugar exudation overflowing during photosynthesis
migdw	$\varphi([Dact:C],[D:C]) = (1-\alpha_1)\frac{\nu}{2}\left[1+tanh\left(\frac{\frac{[Dact:C]}{[Dact:N]}-qC2N}{\delta_{CN}}\right)\right][Dact:C]$	Diatoms downward migration when diatoms internal quota of carbon to nitrogen $\left[\frac{D_{act}:C}{D_{act}:N}\right]$ exceeds a threshold value qC2N
	$\varphi([Dact:N],[D:N]) = (1-\alpha_1)\frac{\nu}{2}\left[1+tanh\left(\frac{\frac{[Dact:C]}{[Dact:N]}-qC2N}{\delta_{CN}}\right)\right][Dact:N]$	
exu_mig1	$\varphi([Dact:C],\infty)_E = \frac{\alpha_1}{1-\alpha_1}\varphi([Dact:C],[D:C])$	Exudation of glyco-proteins during downward migration
	$\varphi([Dact:N],[DON]) = \frac{\alpha_1}{1-\alpha_1}\varphi([Dact:N],[D:N])$	
uptN	$\varphi([DIN],[D:N]) = \frac{\alpha_2}{2}\frac{[DIN]}{[DIN]+K_N}\frac{[D:C]}{[D:C]+K_C}L_T$	Inorganic nitrogen assimilation by inactive diatoms when below mud surface
	$\varphi([DIN],[Dact:N]) = \frac{\alpha_2}{2}\frac{[DIN]}{[DIN]+K_N}\frac{[Dact:C]}{[Dact:C]+K_C}L_T$	Inorganic nitrogen assimilation by active diatoms at the surface
respiration	$\varphi([Dact:C],\infty)_R = \gamma\varphi([DIN],[Dact:N])$	Active and inactive diatoms respiration
	$\varphi([D:C],\infty)_R = \gamma\varphi([DIN],[D:N])$	
migup	If h=0 and E_{PAR}>0	

* Corresponding author: rakotomalala.c@gmail.com

	$\varphi([D:C],[Dact:C]) = (1-\alpha_1)\frac{\nu}{2}\left[1+tanh\left(\frac{\left[\frac{[D:N]}{D:C}\right]-qN2C}{\delta_{CN}}\right)\right][D:C]$ Otherwise $\varphi([D:C],[D_{act}:C]) = 0$	Diatoms upward migration when internal quota of nitrogen to carbon $\left[\frac{D:N}{D:C}\right]$ exceeds a threshold value qN2C and the tide is low during the day
	If h=0 and $E_{PAR}>0$ $\varphi(D:N,Dact:N) = (1-\alpha_1)\frac{\nu}{2}\left[1+tanh\left(\frac{\frac{[D:N]}{[D:C]}-qN2C}{\delta_{CN}}\right)\right][D:N]$ Otherwise $\varphi(D:N,D_{act}:N) = 0$	
exu_mig2	$\varphi([D:C],\infty)_E = \left(\frac{\alpha_1}{1-\alpha_1}\right)\varphi([D:C],[Dact:C])$	Exudation of glyco-proteins during upward migration
	$\varphi([D:N],[DON]) = \left(\frac{\alpha_1}{1-\alpha_1}\right)\varphi([D:N],[Dact:N])$	
mnat1	$\varphi([D:N],[PON]) = \mu_m[D:N]$	Loss of nitrogen pool in inactive diatoms due to natural mortality
mnat2	$\varphi([D:C],\infty) = \mu_m[D:C]$	Loss of carbon pool in inactive diatoms due to natural mortality
diffusion	$\varphi([DIN_{SED}],[DIN]) = D_0\frac{\varphi_d}{\theta^2}\frac{[DIN_{SED}]-[DIN]}{0.01^2}$	Chemical diffusion of nutrients from the second cm depth layer
uptB	$\varphi([DON],[Bact:N]) = \alpha_3\frac{[DON]}{[DON]+K_b}L_T e^{(-\beta_1[DOC])}$	DON assimilation by bacteria
rem1	$\varphi([PON],[DON]) = \alpha_{rem}[PON]e^{[\beta_2(T-T_{opt}{}^B)]}$	Bacterial enzymatic activities transforming PON

* Corresponding author: rakotomalala.c@gmail.com

		into DON
rem2	$\varphi([DON],[DIN]) = \alpha_{rem}[DON]e^{[\beta_2(T-T_{opt}{}^B)]}$	Bacterial enzymatic activities transforming DON into DIN
lysis	$\varphi([Bact:N],[DON]) = \alpha_4[Bact:N]$	Bacteria mortality due to viral lysis
sink	$\varphi([DOC],\infty)_S = \mu[DOC]$	Loss of DOC ex-ported to water column at high tide through hydrolysis and diffusion

934
935
936
937
938
939
940
941
942
943
944

* Corresponding author: rakotomalala.c@gmail.com

945 Table 5: Parameters used in the model

Parameter name	Parameter meaning	Unit	Value	References
K_{PAR}	Light saturation constant	W m^{-2}	100	Guarini et al., 2000
T_{max}	Diatom lethal temperature	°C	38	Blanchard et al. (1996)
T_{opt}	Diatom optimal growth temperature	°C	20	Inspired from Blanchard et al. (1996)
β	Exponential curvature	No unit	0.1	Inspired from Blanchard et al. (1996)
P_{max}	Maximum photosynthetic rate	mol C m^{-3} s^{-1}	120.3 10^{-5}	Guarini et al., 2000
K_1	Photosynthesis half-saturation value of internal pool of nitrogen in active diatoms	mol N m^{-3}	1	Assumed
γ_P	Proportion of photosynthesized carbon overflow as carbohydrate EPS	No unit	0.38	Inspired from Smith and Underwood, 1998
α_1	Proportion of exudation required for vertical migration	No unit	0.05	Inspired from Smith and Underwood, 1998
υ	Maximal migration rate	s^{-1}	0.5	Assumed
q_{C2N}	Maximal value for internal C/N quota in active diatoms	No unit	3.5	Assumed
δ_{CN}	Slope of the sensitivity curve for downward and upward migration	No unit	0.1	Assumed
α_2	Maximum diatom DIN uptake rate	mol N m^{-3} s^{-1}	2 10^{-5}	Assumed
K_N	Diatom DIN uptake half-saturation value for DIN in inactive diatoms	mol N m^{-3}	0.5	Assumed

* Corresponding author: rakotomalala.c@gmail.com

K_C	Diatom DIN uptake half-saturation value for energetic carbon pool in inactive diatoms	mol C m^{-3}	10	Assumed
γ	Stoichiometric proportion of diatoms energetic carbon pool consumed through respiration to uptake DIN	No unit	4	Assumed
q_{N2C}	Minimum value for internal C/N quota in inactive diatoms	No unit	0.7	Assumed
μ_m	Diatoms natural mortality rate	s^{-1}	3 10^{-9}	Assumed
α_3	Maximum DON uptake rate for bacteria	mol N m^{-3} s^{-1}	4.8 10^{-5}	Synthesis based on Degré et al., 2006, Leguerrier et al., 2003, 2004, and Pascal et al. 2009
K_B	Bacteria DON uptake half-saturation value for DON	mol N m^{-3}	0.2	Assumed
β_1	Bacteria DON uptake inhibition factor due to carbohydrate EPS overflow during photosynthesis	No unit	0.1	Assumed
α_{rem}	DIN remineralization rate through bacterial enzymatic activity	s^{-1}	4.63 10^{-7}	Assumed
β_2	Temperature sensitivity parameter of bacterial enzymatic activity	No unit	0.0405	Ory, 2010 and Ory et al. (2011)
T_{opt}^{B}	Optimal temperature of bacterial enzymatic activity	°C	30	Ory, 2010 and Ory et al. (2011)
α_4	Bacterial mortality rate	s^{-1}	3 10^{-5}	Ory, 2010 and Ory et al. (2011)
μ	DOC resuspension rate	s^{-1}	8 10^{-4}	Assumed
D0	Diffusivity coefficient	m^{-2} s^{-1}	1.4 10^{-9}	Lavery et al., 2001
φ_d	Sediment porosity	No unit	0.89	Measured
θ^2	Tortuosity of the sediment	No unit	1.11	Chatelain, 2010
C:chl *a*	Carbon and chl *a* ratio	mgC mg chl *a*	45	Guarini et al., 2000
Glucose:C	Glucose and carbon ratio	g Glucose gC^{-1}	15	Calculated

946

* Corresponding author: rakotomalala.c@gmail.com

947 ***Bibliography of the appendix***

948 Blanchard, G.F., Guarini, J.M., Richard, P., Gros, P., Mornet, F., 1996. Quantifying the short-
949 term temperature effect in light-saturated photosynthesis of intertidal microphytobenthos.
950 Mar. Ecol. Prog. 134, 309–313.

951 Chatelain, M., 2010. Flux dissous à l'interface eau-sédiment sous des écoulements oscillants.
952 PhD dissertation. Université Pierre et Marie Curie.

953 Degré, D., Leguerrier, D., du Chalet, A.E., Rzeznik, J., Auguet, J., Dupuy, C., Marquis, E.,
954 Fichet, D., Struski, C., Joyeux, E., Sauriau, P., Niquil, N., 2006. Comparative analysis of
955 the food webs of two intertidal mudflats during two seasons using inverse modelling :
956 Aiguillon Cove and Brouage Mudflat, France. Estuar. Coast. Shelf Sci. 69, 107–124.

957 Guarini, J.M., Blanchard, G.F., Gros, P., Gouleau, D., Bacher, C., 2000b. Dynamic model of
958 the short-term variability of microphytobenthic biomass on temperate intertidal mudflats.
959 Mar. Ecol. Prog. Ser. 195, 291–303.

960 Lavery, P.S., Oldham, C.E., Ghisalberti, M., 2001. The use of fick's first law for predicting
961 porewater nutrient fluxes under diffusive conditions. Hydrol. Process. 15, 2435–2451.

962 Leguerrier, D., Niquil, N., Boileau, N., Rzeznik, J., Sauriau, P., Le Moine, O., Bacher, C., 2003.
963 Numerical analysis of the food web of an intertidal mudflat ecosystem on the Atlantic coast
964 of France. Mar. Ecol. Prog. 246, 17–37.

965 Ory, P., 2010. Interactions entre les virus, les flagellés et les bactéries au sein du réseau
966 microbien planctonique du bassin de Marennes-Oléron. PhD dissertation. Université de la
967 Rochelle.

968 Ory, P., Palesse, S., Delmas, D., Montanié, H., 2011. *In situ* structuring of virioplankton through
969 bacterial exoenzymatic activity : interaction with phytoplankton. Aquat. Microb. Ecol. 64,
970 233–252.

971 Pascal, P.-Y., Dupuy, C., Richard, P., Mallet, C., du Châtelet, E.A., Niquil, N., 2009. Seasonal
972 variation in consumption of benthic bacteria by meio- and macrofauna in an intertidal
973 mudflat. Limnol. Oceanogr. 54, 1048–1059.

974 Smith, D.J., Underwood, G.J.C., 1998. Exopolymer production by intertidal epipelic diatoms.
975 Limnol. Oceanogr. 43, 1578–1591.

** Corresponding author: rakotomalala.c@gmail.com*

Supplementary Material SM1

Fig. 1: Simulated MPB concentration (lines) in the first centimeter of sediment under three different types of diffusion: chemical diffusion (A), bio-diffusion 5 times (B) and 10 times (C) greater than the chemical diffusion and under two other MPB initial state: (D:C/D:N)init. = 1 (II) and (D:C/D:N)init. = 0.05 (III). Points correspond to MPB biomass from the study of Orvain et al. (2003). Gray line represents dark immersion periods in the system

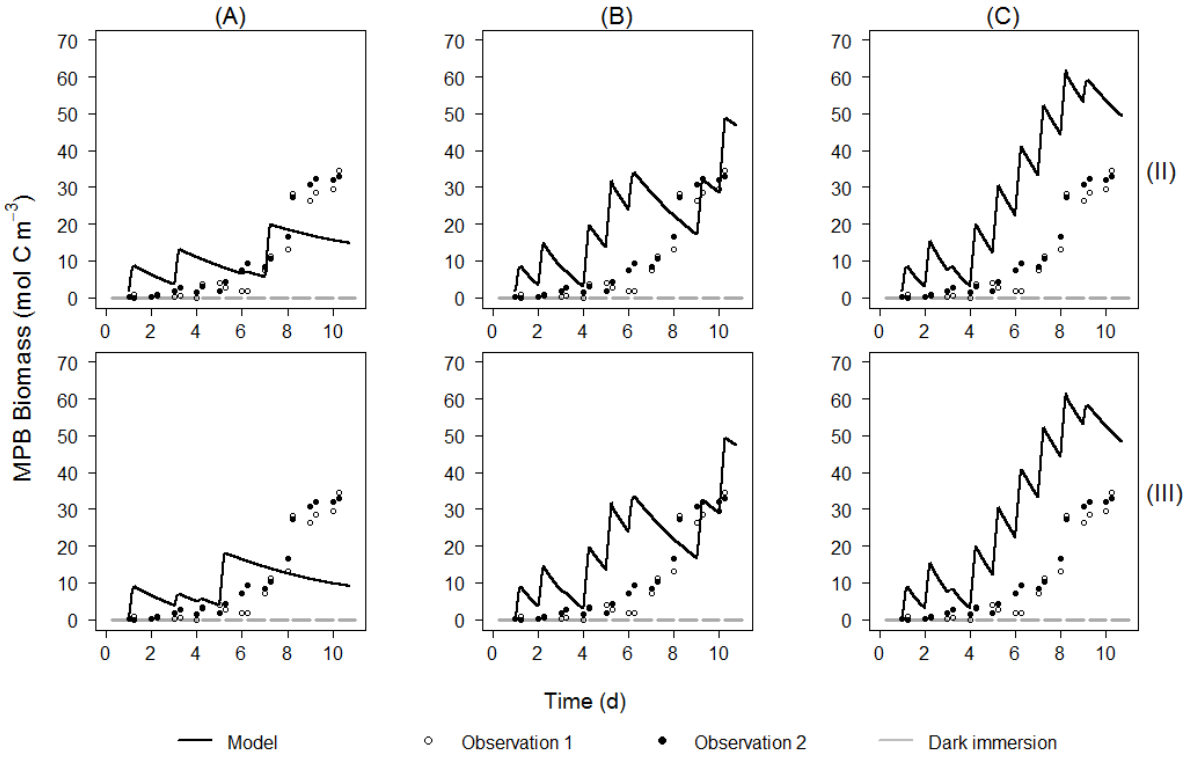

* Corresponding author: rakotomalala.c@gmail.com

Fig. 2: Taylor diagram showing the difference between observed and simulated MPB under different diffusion and different initial state.

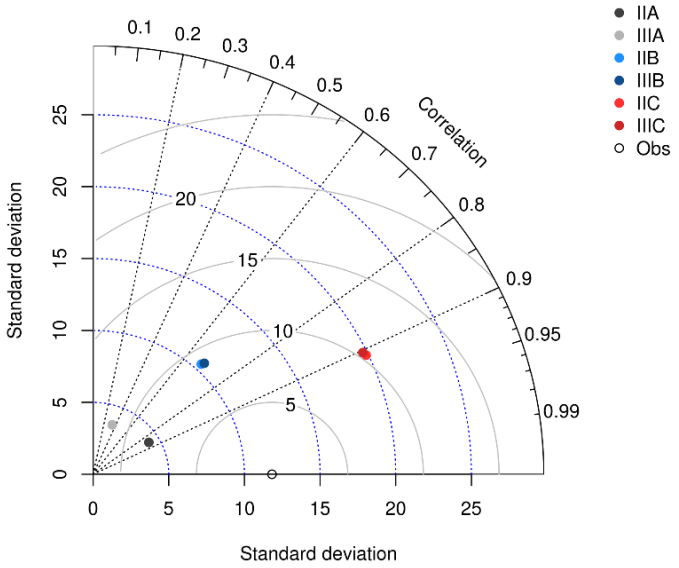

* Corresponding author: rakotomalala.c@gmail.com

Supplementary Material SM2

Fig. 1: Taylor diagram showing the difference between the observed and simulated MPB when different values of qC2N and qN2C were tested.

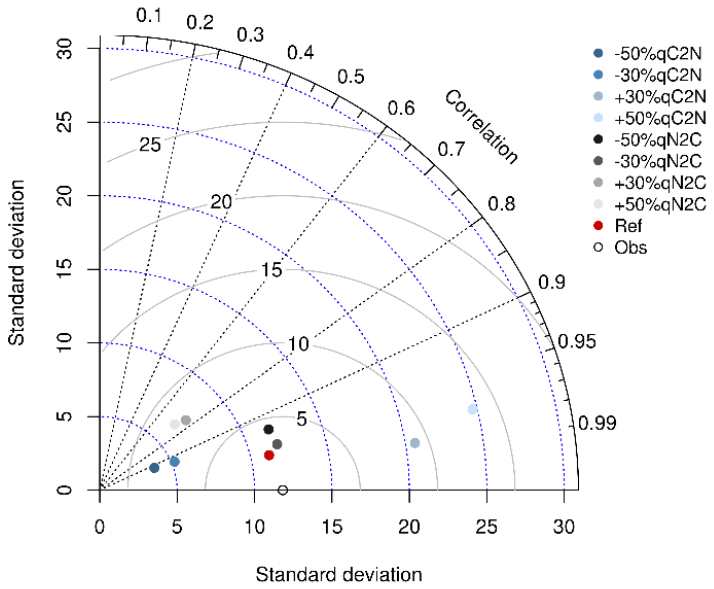

Fig. 2: Taylor diagram showing the difference between the simulated MPB of reference and simulated MPB when different values of qC2N and qN2C were tested.

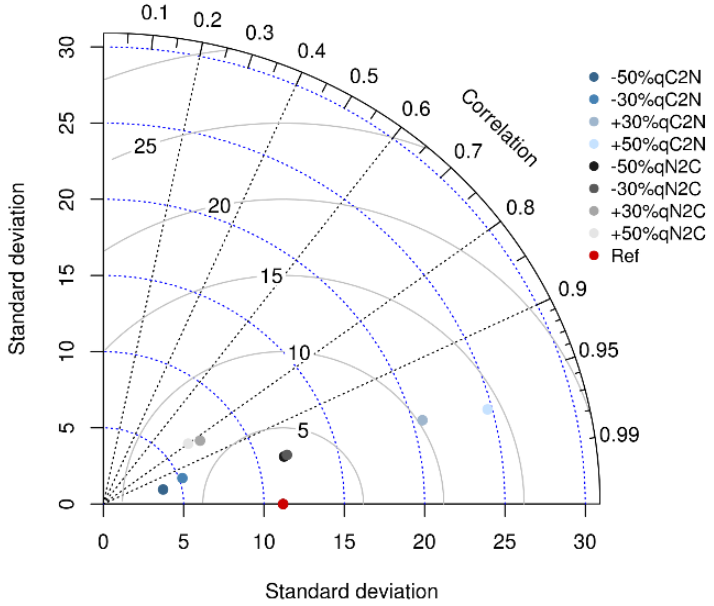

* Corresponding author: rakotomalala.c@gmail.com